UNIVERSITY of York

This is a repository copy of *Insect egg-induced physiological changes and transcriptional reprogramming leading to gall development*.

White Rose Research Online URL for this paper:
https://eprints.whiterose.ac.uk/167880/

Version: Accepted Version

Article:

Oates, Caryn N., Denby, Katherine orcid.org/0000-0002-7857-6814, Myburg, Alexander A. et al. (2 more authors) (2020) Insect egg-induced physiological changes and transcriptional reprogramming leading to gall development. Plant, Cell and Environment. ISSN 0140-7791

https://doi.org/10.1111/pce.13930

Reuse
Items deposited in White Rose Research Online are protected by copyright, with all rights reserved unless indicated otherwise. They may be downloaded and/or printed for private study, or other acts as permitted by national copyright laws. The publisher or other rights holders may allow further reproduction and re-use of the full text version. This is indicated by the licence information on the White Rose Research Online record for the item.

Takedown
If you consider content in White Rose Research Online to be in breach of UK law, please notify us by emailing eprints@whiterose.ac.uk including the URL of the record and the reason for the withdrawal request.

White Rose
university consortium
Universities of Leeds, Sheffield & York

eprints@whiterose.ac.uk
https://eprints.whiterose.ac.uk/

1 **Insect egg-induced physiological changes and transcriptional reprogramming leading to gall formation**

2

3 Caryn N. Oates [1], Katherine J. Denby [2], Alexander A. Myburg [1], Bernard Slippers [1] and Sanushka Naidoo [1]

4

5 [1]Department of Biochemistry, Genetics and Microbiology, Forestry and Agricultural Biotechnology

6 Institute (FABI), University of Pretoria, Private Bag x20, Pretoria 0028, South Africa

7 [2]Department of Biology, University of York, Wentworth Way, York YO10 5DD, UK;

8 katherine.denby@york.ac.uk

9

10 Corresponding author: Sanushka Naidoo

11 sanushka.naidoo@up.ac.za

12 +27 12 420 4974

13

14

Abstract

Gall-inducing insects and their hosts present some of the most intricate plant-herbivore interactions. Oviposition on the host is often the first cue of future herbivory and events at this early time point can affect later life stages. Many gallers are devastating plant pests, yet little information regarding the plant-insect molecular interplay exists, particularly following egg deposition. We studied the physiological and transcriptional responses of *Eucalyptus* following oviposition by the gall-inducing wasp, *Leptocybe invasa*, to explore potential mechanisms governing defence responses and gall development. RNA sequencing and microscopy were used to explore a susceptible *Eucalyptus-L. invasa* interaction. Infested and control material was compared over time (1-3, 7 and 90 days post oviposition) to examine the transcriptional and morphological changes. Oviposition induces accumulation of ROS and phenolics which is reflected in the transcriptome analysis. Gene expression supports phytohormones and ten transcription factor subfamilies as key regulators. The egg and oviposition fluid stimulate cell division resulting in gall development. *Eucalyptus* responses to oviposition are apparent within 24 hours. Putative defences include the oxidative burst and barrier reinforcement. However, egg and oviposition fluid stimuli may redirect these responses towards gall development.

Keywords: Developmental regulation, *Eucalyptus*, gall insect, *Leptocybe invasa*, oviposition, plant cell redifferentiation, plant defence, transcription factor

35 **Introduction**

36

37 Plants and insects have co-existed for hundreds of millions of years whichh has led to a wide variety of
38 interactions between these organisms (Erb & Reymond, 2019). One of the most intricate relationships is
39 the ability of some insect species to deposit their eggs and induce galls on their hosts. Galls are abnormal
40 plant growths that are formed by active redifferentiation of plant tissues and provide the developing
41 insect with superior nourishment and protection (Stone & Schönrogge, 2003). To defend themselves,
42 plants have evolved a complex immune system comprising constitutive and inducible components.
43 Constitutive defences are preformed physical or chemical barriers with insecticidal or antixenotic activity,
44 whilst inducible defences are activated following recognition of elicitors (Jones & Dangl, 2006; Erb &
45 Reymond, 2019).

46

47 In many cases, plant-galling insect interactions begin with oviposition on the host (Reymond, 2013). The
48 site of egg deposition, including the accompanying oviposition fluid, on the leaf surface is an important
49 interface where the first cues of imminent herbivory are perceived (Hilker & Fatouros, 2015). Different
50 molecules may be recognised by the plant leading to the onset of induced immune responses, including
51 herbivore-, egg- and damage-associated molecular patterns (HAMPs, EAMPs and DAMPs, respectively) as
52 well as effectors (Boller & Felix, 2009; Hogenhout & Bos, 2011; Stuart, 2015). The latter are compounds
53 secreted by the pest that mitigate the plant immune system and manipulate host physiology via specific
54 host targets and are hypothesised to play key roles in plant-galling insect interactions (Deslandes & Rivas,
55 2012, Oates *et al.*, 2016). However, few causative molecules have been characterised in insect eggs or
56 oviposition fluids, particularly for gall-inducing species.

57

58 Recognition is linked to the downstream defences by signalling machinery. Phytohormones, especially
59 jasmonic acid (JA), salicylic acid (SA) and ethylene (ET), play central roles in organising defence against
60 biotic stresses (Berens *et al.*, 2017). There is extensive crosstalk between hormone signalling pathways
61 which provides a means of tailoring the immune system to the appropriate response (Erb *et al.*, 2012). JA
62 is considered to be the primary regulator of plant resistance against insect herbivory (Erb & Reymond,
63 2019) as well as responses to egg deposition and associated wounding (Reymond, 2013). Up-regulation
64 of JA biosynthesis- or signalling-related genes has been reported in response to oviposition by numerous
65 insect species as well as EAMP treatment (Little *et al.*, 2006; Büchel *et al.*, 2012; Oates *et al.*, 2015) and is
66 associated with increased egg mortality (Ament *et al.*, 2004).

67

68 Pest perception by a plant can cause extensive local cellular reprogramming aimed at neutralising the
69 threat by direct and indirect defence mechanisms (Fürstenberg-Hägg *et al.*, 2013). Direct defences involve
70 the synthesis of toxic compounds that act directly on the pest, whilst indirect defences involve the release
71 of volatile signatures that attract the natural enemies of the pest (Unsicker *et al.*, 2009; Fürstenberg-Hägg
72 *et al.*, 2013). A relatively small number of studies have examined plant responses to insect egg deposition,
73 with fewer examining those induced by gallers. An array of defences has been reported in these studies
74 including neoplasm development (Doss *et al.*, 2000) and production of larvicidal or ovicidal compounds
75 (Fatouros *et al.*, 2015) as well as the release of volatile compounds that attract egg and/or larval
76 parasitoids (Hilker *et al.*, 2002). Studies exploring plant resistance against galling insects have
77 predominantly focused on larval life stages. To our knowledge, only one study has demonstrated induced
78 terpene and transcriptome changes in response to the gall-inducing blue gum chalcid wasp (*Leptocybe*
79 *invasa*) oviposition on *Eucalyptus* (Oates *et al.*, 2015).

80

81 The most commonly reported response to oviposition is the elicitation of a hypersensitive response (HR)
82 (Hilker & Fatouros, 2016). The HR is preceded by a burst of reactive oxygen species (ROS) that induces the
83 expression of pathogenesis-related (*PR*) genes and localised cell death at the site of egg deposition causing
84 desiccation, detachment or is directly ovicidal (Balbyshev & Lorenzen, 1997; Geuss *et al.*, 2017; Griese *et*
85 *al.*, 2017). ROS, along with effectors and phytohormones, have been proposed as important role players
86 in gall initiation and development (Isaias *et al.*, 2015). The eggs and oviposition fluid of some galling
87 species have been shown to stimulate redifferentiation and proliferation of adjacent host cells within days
88 of deposition and occur alongside necrotic zones (Leggo & Shorthouse, 2006; Sliva & Shorthouse, 2006;
89 Barnewall & de Clerck-Floate, 2012). This suggests that the pre-larval life stage is involved in the initiation
90 of gall development. There is currently no comprehensive, molecular model that offers biological insight
91 for any plant-galling insect species interaction. Future studies that clarify the mechanisms that govern
92 resistance versus susceptibility will be imperative for the development of effective control measures
93 against these pests.
94
95 *Leptocybe invasa* Fisher & La Salle (Hymenoptera: Eulophidae) is a gall-inducing pest of numerous,
96 economically valuable *Eucalyptus* species and has achieved a global distribution since its discovery in 2000
97 (Mendel *et al.*, 2004; Dittrich-Schröder *et al*., 2018). It preferentially oviposits on immature shoot tips,
98 midribs and petioles where successful larvae induce the formation of coalescing galls that may cause
99 stunting, die-back or death (Mendel *et al.*, 2004). We previously examined the transcriptional
100 reprogramming and induced changes in the terpene profile of resistant and susceptible *Eucalyptus*
101 genotypes in response to *L. invasa* oviposition at seven days post infestation (dpi) (Oates *et al.*, 2015). This
102 study showed that expression of genes associated with phytohormones, direct and indirect defences was
103 altered in response to *L. invasa* oviposition. A study by Li *et al.*, (2017) explored concentration dynamics
104 of selected compounds during *L. invasa*-induced gall development from oviposition to maturity. The study

105 examined the levels of carbon, nitrogen, phenolics, tannins and four phytohormones (auxins, cytokinins,
106 gibberellins (GA) and abscisic acid (ABA)) in two *Eucalyptus* genotypes varying in susceptibility to the gall
107 wasp. Interestingly, the results of the metabolite analysis at the pre-larval stage are reflected in the
108 transcriptomic responses described by Oates *et al.*, (2015).
109
110 Our previous study confirmed that the host *Eucalyptus* can identify the blue gum chalcid oviposition and
111 elicit defences that included alterations to the terpene profile. However, there is no information available
112 on the basic biology of the interaction such as where the egg and oviposition fluid are positioned or what
113 transcriptional and anatomical changes are induced that lead to gall formation. In this study, we
114 investigated *L. invasa* oviposition-induced physical and transcriptional responses of a susceptible
115 *Eucalyptus* hybrid clone over time.
116
117 **Materials and Methods**
118
119 *Infestation trial*
120
121 Two-year-old ramets of a susceptible (Dittrich-Schröder *et al.*, 2012) *Eucalyptus grandis* x *Eucalyptus*
122 *camaldulensis* hybrid clone (GC 540, Mondi) were coppiced and regrown in a *L. invasa*-proof field cage
123 insectarium. Ramets were divided into control and infested groups. For infested samples, newly emerged
124 *L. invasa* adults were collected in groups of five and exposed to selected target sites, which included the
125 shoot tip, the subsequent two immature leaves (≤ 3 cm in length) and the petiole at three target sites per
126 ramet (Figure 1). These sites were selected because they represent tissue that is preferentially targeted
127 by the gall wasp. A small plastic sleeve was tied around the target material to prevent wasp escape. The
128 wasps could oviposit from 11:00 to 12:00 before removal to ensure minimal diurnal variation was

129 introduced into the experiment. Control samples were not exposed to *L. invasa* but were otherwise
130 treated equivalently. For transcriptome analysis, material was collected at 1, 2 and 3 dpi at 12:00 and
131 immediately frozen in liquid nitrogen. Each time point included three biological replicates of control and
132 infested samples. Each replicate was made up of material collected from three ramets. For microscopy
133 analysis, material was collected at 1 hour post infestation (hpi) as well as 1, 2, 3, 7 and 90 dpi in triplicate
134 as described for the transcriptomics.
135
136 *Fixation and staining*
137
138 For light microscopy, excised oviposition sites were fixed in formaldehyde, acetic acid and 50% ethanol
139 (FAA, 1:1:18) (Berlyn *et al.*, 1976) and dehydrated in a butanolic series. Dehydrated samples were
140 embedded in paraffin wax (Sigma-Aldrich), sectioned with a rotary microtome (10 µm) and attached to
141 slides using Haupt's adhesive (1 g gelatine, 2 g phenol, 15 ml glycerine, 100 mL H_2O). Wax was removed
142 using 100% xylene prior to staining. Sections were dual stained with Safranin O (uniLAB) and Fast Green
143 FCF (uniLAB) before mounting in Entellan (Merck Millipore). The sections were photographed using a Carl
144 Zeiss AG Axiocam ICc3 digital camera (Oberkochen, Germany) coupled to a light microscope (Carl Zeiss AG
145 Axioskop) using Carl Zeiss AG AxioVision SE64 v4.9.0.0 software.
146
147 To measure H_2O_2 accumulation, whole infected and non-infected leaves were submerged in 3,3'-
148 Diaminobenzidine tetrahydrochloride (DAB) Liquid Substrate solution (Sigma-Aldrich) for 4 hours. Leaves
149 were destained by boiling in bleaching solution (ethanol, glacial acetic acid and glycerol, 3:1:1) at 95°C for
150 40 minutes and stored at 4°C. Leaves were photographed using an Olympus DP21 digital camera
151 (Massachusetts, USA) coupled to a Nikon SMZ1500 dissecting microscope (Nikon Corp., Tokyo, Japan)
152 using Olympus Stream Basic v1.9.4 software.

153

154 *RNA isolation and sequencing*

155

156 Infested and control samples were collected and immediately frozen in liquid nitrogen. Material was
157 excised approximately 5 mm around the oviposition sites whilst ensuring minimal thawing (Figure 1A).
158 The shoot tips, lower section of the midribs and petiole (the prospective oviposition sites) were excised
159 for control samples (Figure 1B, C). For 1 and 2 dpi control samples, these tissues were pooled (Figure 1B).
160 For the 3 dpi, these tissues were kept separately (Figure 1C). Total RNA was extracted using the Norgen
161 Plant/Fungi Total RNA Purification Kit (Norgen Biotek Corp.). Samples were treated using Qiagen RNase-
162 free DNase I enzyme (Qiagen Inc., Valencia, California, USA) and purified using the Qiagen RNeasy Mini
163 Kit and following the manufacturer's instructions. The concentration and quality of the RNA samples was
164 tested using the Bio-Rad Experion analyser (Bio-Rad, Hercules, USA). Total RNA was submitted to Beijing
165 Novogene Technology Co. Ltd. (Beijing, China) for mRNA-Seq analysis. The RNA libraries were prepared
166 using the TruSeq Stranded mRNA Library Prep Kit (Illumina Inc., San Diego, California, USA) with a 300 bp
167 insert. Samples were sequenced on the Illumina HiSeq 2500 platform in two batches with PE150 and
168 PE125 reads, respectively.

169

170 *Read mapping to the Eucalyptus v2.0 genome*

171

172 Read quality was analysed using FastQC v0.11.3 (Andrews 2010) and reads were trimmed using
173 Trimmomatic v0.32 (Bolger *et al.*, 2014) to ensure the mean and interquartile range per base sequence
174 quality scores were above a Phred score of 30 and the per base sequence content was passed. Reads were
175 aligned to the *E. grandis* v2.0 reference genome (Myburg *et al.*, 2014) using Tophat2 v2.0.14 (Kim *et al.*,
176 2013) and summarised using FeatureCounts v1.5.0-p3 (Liao *et al.*, 2014). DESeq2 v1.12.4 (Love *et al.*,

177 2014) was used to normalise the read counts using variance stabilising transformation and identify
178 significantly differentially expressed genes (DEGs) in infested versus control samples (adjusted p-value ≤
179 0.001) at each time point. DEGs at 3 dpi were calculated as infested versus all controls (ie. [INF] versus
180 [ST, MR, PT]). DEGs were filtered for $\log_2$ fold changes ≥ 1.00 and ≤ -1.00 prior to further analysis. Data
181 will be made available at https://eucgenie.org/.
182
183 *Gene Ontology enrichment*
184
185 Gene Ontology (GO) functional enrichment of up- and down-regulated DEGs was calculated with Fisher's
186 exact test using all *E. grandis* v2.0 genes as a reference; p-values were corrected for multiple testing using
187 the Benjamini and Hochberg false discovery rate (FDR) method (Benjamini & Hochberg, 1995). A corrected
188 p-value of < 0.05 was used as a threshold to select enriched terms or pathways. The same approach was
189 used to identify GO enrichment in network modules.
190
191 *Transcription factor family analysis*
192
193 Gene expression was analysed for 248 DEGs classified as TFs in the Plant Transcription Factor Database
194 v4.0 (Jin *et al.*, 2014, 2015, 2017) and grouped by subfamily as defined by their associated *Arabidopsis*
195 *thaliana* orthologues. Subfamilies overrepresented (adjusted p-value < 0.05) for DEGs at each time point,
196 using all *E. grandis* v2.0 genes as a reference, were identified using the hypergeometric distribution with
197 FDR correction (Benjamini & Hochberg, 1995).
198
199 *Co-expression network modelling*
200

201 Members of enriched TF subfamilies at the respective time point were selected as baits for gene co-
202 expression network generation (Supplementary File S4.4). The analysis utilised an expression matrix
203 incorporating data for all samples in this study as well as publicly available, pre-processed transcriptomic
204 data from three prior studies of *Eucalyptus* biotic stress responses (https://eucgenie.org), including
205 infection by *Phytophthora cinnamomi* (Meyer *et al.*, 2016), *Chrysoporthe austroafricana* (Mangwanda *et*
206 *al.*, 2015) and infestation by *L. invasa* (Oates *et al.*, 2015). The co-expression network was generated using
207 CoExpNetViz v1.0.2 (Tzfadia *et al.*, 2016) using the Pearson correlation coefficient method and filtered to
208 include positive relationships between DEGs in the 95th percentile. Functional modules were identified
209 using the MCL Cluster network partitioning algorithm from clusterMaker2 v1.2.1 (Morris *et al.*, 2011).
210 Downstream modifications were completed using Cytoscape v3.6.1 (Shannon *et al.*, 2003).
211
212 *Transcription factor binding site analysis*
213
214 For transcription factor binding site (TFBS) analysis, 1500 bp upstream of the transcriptional start site of
215 the network members was extracted. Sequences were filtered to ensure the promoter region did not
216 overlap with preceding or succeeding genes and ≥100 bp in length. AME (Analysis of Motif Enrichment)
217 v5.0.5 (http://meme-suite.org/) was used to identify known, enriched *Arabidopsis thaliana* motifs (E-
218 value ≤ 0.0001, network cluster membership relative to whole genome) in the promoters as this is not
219 currently available for *Eucalyptus*.
220
221 **Results**
222
223 *Oviposition-induced cellular responses enable* L. invasa *gall development*
224

225 Adult *L. invasa* females oviposit along the main vein on the ventral side of the plant tissue (Figure 2A, B
226 and Supplementary file S1). Scarring is apparent within one hour (1 hpi) of egg deposition and becomes
227 increasingly pronounced over time (Figure 2A and Supplementary file S1). ROS accumulation is co-
228 localised with the wound sites and increases in concentration from 1 to 3 dpi and appears stable until at
229 least 7 dpi (Figure 2A1-A5 and Supplementary file S1).
230
231 During each oviposition event, a channel is cut by the ovipositor and a single egg and oviposition fluid is
232 deposited into/near the plant vasculature (Figure 2B3-B5 and Supplementary file S1). The oviposition fluid
233 has a strong degradative effect on the surrounding tissue with cells showing thin/degraded cell walls
234 within an hour of exposure (Figure 2B3, B4) and is sustained over seven days. The newly laid egg is round
235 and possesses a long pedicel for anchorage (Figure 2B5). At 1-3 dpi, the developing embryo becomes
236 elongated and is roughly aligned with the vascular tissue vessels (Figure 2B6-B8). We also observed the
237 accumulation of phenolic compounds in the ventral cells at 1 dpi which was maintained over the entire
238 time series (Figure 2B6-B9, B11, B13). The phenolics appear to be co-localised with the ROS and the
239 oviposition-induced scarring (Figure 2A relative to Figure 2B and Supplementary file S1). At 7 dpi, there is
240 a clearly defined area of cell division parallel to the spread of the oviposition fluid in the host tissues
241 (Figure 2B9, B10). Where eggs are visible in the vasculature, cell division radiates outward from the egg
242 and a zone of redifferentiated tissue is apparent around these sites (Figure 2B9, B11, B12). Additionally,
243 the embryo is located in an immature gall chamber (Figure 2B12). Finally, we compared the structure of
244 the gall at 90 dpi to published results to confirm that the artificial infestation approach results in the
245 structure described by Isaias *et al.* (2018). At this stage, the larva has established a mature gall comprising
246 three distinct layers including nutritive tissue that forms the innermost lining of the chamber, followed by
247 a lignified sheath and oxalate crystal deposits (Figure 2B13). The nutritive tissue is approximately six cell
248 layers thick and cells possess a dense, granular cytoplasm (Figure 2B13).

249

250 *Expression analysis shows defence response*

251

252 Having seen rapid changes in the host physiology, we then investigated the transcriptional responses of
253 the host following *L. invasa* infestation. Whole genome expression profiles were obtained from high-
254 quality *Eucalyptus* RNA (Table S1). The same tissue types that were used to examine the physical
255 interaction between *L. invasa* and *Eucalyptus* were used for RNA extraction. Sequencing of the samples
256 yielded a minimum of 4.68×10^7 reads per sample with 81-97% mapped. DESeq2 analysis identified 2140,
257 1003 and 1193 genes showing significant differential expression between control and infested samples at
258 1, 2 and 3 dpi, respectively (Supplementary File S2). In each case more genes showed up-regulated
259 expression than down-regulated.

260

261 At 1 dpi, up-regulated genes are enriched for defence-related GO terms including phytohormone-
262 mediated signalling pathways, oxidative stress and secondary metabolism (Figure 3A). Responses to
263 abscisic acid (ABA) and JA are prevalent, particularly ABA and JA which are enriched throughout the series
264 (Figure 3A1). The observation that genes related to ABA and JA signalling are apparent over the time
265 points suggests that these hormones may act as important regulators of the plant defence response
266 against this pest. Responses to auxin and ethylene (ET) as well as biosynthesis of ET and JA are apparent
267 at 1 dpi, whilst responses to salicylic acid (SA) are apparent at 3 dpi (Figure 3A1). There is also a sustained
268 response to oxidative stress over all three time points suggesting that the plant-type hypersensitive
269 response may be involved which corresponds to the observed ROS accumulation at oviposition sites
270 (Figure 3A2). Similarly, up-regulation of phenylpropanoid biosynthesis-related genes corresponds to the
271 increasing concentration of phenolic compounds (Figure 3A3). GO terms related to the biosynthesis or
272 response to phenolic derivatives are also observed here. Further analysis of phenylpropanoid biosynthetic

273 genes revealed up-regulation of the pathway, particularly leading to the synthesis of lignin monomers,
274 consistently from 1 dpi to 3 dpi (Figure 3B).
275
276 The GO terms also indicate a down-regulation of genes relating to growth and development such as cell
277 proliferation at 1 dpi (Figure 3A4). Additionally, we observe up-regulation of carbohydrate metabolism
278 and nitrate transport (Figure 3A4). Finally, the enriched GO terms also suggest cellular processes that may
279 promote host susceptibility including up-regulation of toxin catabolism suggesting a decrease in the
280 concentration of insecticidal chemicals in the proximal tissues. The former may also contribute to defence
281 by enabling the breakdown of insect-secreted toxins.
282
283 *Ten transcription factor subfamilies show enrichment at 1 dpi*
284
285 We identified 248 differentially expressed TF-encoding genes (Supplementary File S3) across the time
286 points that are putatively involved in regulating the *Eucalyptus* responses to oviposition. We further
287 tested whether specific subfamilies of TFs were up- or down-regulated at coordinated times following
288 oviposition. Here we consider orthologous genes that share a common *A. thaliana* annotation as
289 individual members of a TF subfamily. Ten subfamilies, comprising 40 up-regulated genes, showed
290 enrichment at 1 dpi (adjusted p-value ≤ 0.05), including *EgrATAF1, EgrMYB15, EgrMYB36, EgrMYB102*,
291 *EgrMYC2*, *EgrRAP2.1, EgrRAP2.6L, EgrWRKY28*, *EgrWRKY6* and *EgrWRKY75* (Figure 4).
292
293 *Co-expression and transcription factor binding site enrichment analyses reveal putative biological*
294 *pathways regulated by transcription factors*
295

296 We investigated biological processes that may be regulated by the TFs and putatively contribute to gall
297 development. The 40 DEGs belonging to the ten enriched TF subfamilies were used as baits to generate a
298 co-expression network. The expression matrix encompassed data from this study and from publicly
299 available *Eucalyptus*-biotic stress transcriptome analyses including responses to fungus (*C.*
300 *austroafricana*), oomycete (*P. cinnamomi*) and *L. invasa*. The network includes genes that were co-
301 expressed with the bait genes and were differentially expressed in this study to reduce noise. The network
302 comprises 656 nodes and 3003 edges (maximum correlation ≥0.8) displayed as Cytoscape's prefuse force
303 directed layout (Figure 5). Two functional modules, comprising 75% of the network nodes, were identified
304 suggesting related functionality between cluster members, which was supported by GO term enrichment.
305 The remainder of the network includes small clusters (≤15 nodes) that do not show enrichment for GO
306 terms or TFBS but may be regulated by their local bait TFs.
307

308 Module 1 (Figure 5, teal) is the largest in the network and is enriched for defence-associated GO terms.
309 These include responses to ABA, SA, ET and JA, the oxidative burst, phenylpropanoid biosynthesis and
310 systemic acquired resistance. This module includes up-regulated phenylpropanoid biosynthetic genes
311 (orange nodes) observed in Figure 2B as well as several pathogenesis-related such as *EgrPR1* and *EgrPR4*
312 which are markers of the SA and JA pathways, respectively. Module 1 also comprises 25 of the enriched
313 TF subfamily members, including *EgrATAF1, EgrMYB15, EgrMYB36, EgrMYB120, EgrMYC2, EgrWRKY6,*
314 *EgrWRKY28, EgrWRKY75, EgrRAP2.1* and *EgrRAP2.6L* suggesting that they may regulate similar biological
315 processes or that a higher resolution of data is needed to distinguish which processes are regulated by
316 the TFs. TFBS enrichment analysis identified enriched motifs (*A. thaliana*) in this module including NAC
317 and WRKY highlighting possible binding sites for the bait genes *ATAF1*, *WRKY6*, *WRKY28* and *WRKY75*
318 (Figure 5) further supporting the putative regulatory role of these TFs in the response.
319

320 Module 2 (Figure 5, light green) includes four *EgrMYB102* bait genes and one *EgrMYB36*. Interestingly,
321 three of the baits are exclusively differentially expressed following *L. invasa* oviposition on resistant and
322 susceptible host genotypes based on this study and currently available datasets (Mangwanda *et al.*, 2015;
323 Oates *et al.*, 2015; Meyer *et al.*, 2016). These baits are co-expressed with 73 genes where 83% of them
324 only show differential expression in response to *L. invasa* from this study and/or Oates *et al.* (2015) but
325 not other *Eucalyptus*-biotic stress interactions (Supplementary File S4) and are enriched for responses to
326 nitrate and lipid transport, suggesting a specific role in response to *L. invasa*. This cluster also showed
327 enrichment for MYB TFBSs suggesting a regulatory role for *EgrMYB36* and *EgrMYB102* in this module
328 (Supplementary File S5). The results suggest that this module may play an important role in the *Eucalyptus*
329 response to the gall wasp.
330
331 **Discussion**
332
333 This study investigated the *L. invasa* oviposition-induced responses of *Eucalyptus* over time. Physiological
334 responses are apparent within one hour of egg deposition and include scarring, ROS accumulation and
335 plant cell lysis putatively caused by the oviposition fluid. Extensive transcriptional reprogramming is
336 apparent at the earliest time point of 1 dpi. DEGs are enriched for defence- and gall development-related
337 biological processes, many of which are reflected in the histological analysis. Results suggest that the
338 phytohormones JA and ABA as well as ten TF subfamilies may play important regulatory roles in this
339 interaction. Members of these TF subfamilies (40 genes in total) were co-expressed with genes that were
340 divided into two modules and ten gene clusters or individuals putatively involved in defence and gall
341 development. The modules also showed enrichment of TFBSs, including *NAC, WRKY* and *MYB*, which
342 supports the regulatory role of these TFs in the *Eucalyptus-L. invasa* interaction. Finally, we show the co-
343 occurrence of phenolics, ROS and auxin transcriptional responses, which are essential components for gall

344 development, suggesting that the *L. invasa* egg and oviposition fluid are responsible for initiating galling
345 in this system.
346
347 *Leptocybe gall induction*
348
349 ROS accumulation is apparent here within one hour of *L. invasa* oviposition and increases over time
350 (Figure 2A). Gene enrichment and up-regulation of certain key genes in the time series, such as respiratory
351 burst oxidase homologs D and F (*EgrRBOHD, EgrRBOHF*), support the onset of the defence-related
352 oxidative burst (Gouhier-Darimont *et al.*, 2013). Furthermore, *WRKY75* was shown to be involved in ROS
353 accumulation leading to leaf senescence (Guo *et al.*, 2017) and increased resistance to *Xanthomonas*
354 *campestrix* in cabbage (Choi *et al.*, 2016). However, no ovicidal effects manifest and continued embryonic
355 development and gall initiation are observed. Interestingly, *RBOHD* is also commonly up-regulated in
356 plant-galling insect interactions (Takeda *et al.* 2019) suggesting that its function in ROS generation is
357 necessary for galling. ROS participate in numerous biological processes, including cell division and cell wall
358 modification (Considine & Foyer, 2014). Isaias *et al.* (2015) proposed that gall-inducing insects can redirect
359 the defence-related oxidative burst towards cell wall modification to facilitate gall development.
360
361 We demonstrate accumulation of phenolics and up-regulation of the phenylpropanoid biosynthetic
362 pathway genes from 1 dpi at the oviposition site. This pathway is an important source of anti-oxidant
363 molecules, cell wall components and secondary metabolites commonly found in galled tissues (Bedetti *et*
364 *al.*, 2014; Suzuki *et al.*, 2015; Hall *et al.*, 2017). Finally, genes involved in auxin signalling, such as auxin-
365 responsive GH3- and SAUR-like auxin-responsive protein-encoding genes, show differential expression
366 within 1 dpi and are also observed in module 1. These genes are co-expressed with several cell wall
367 modifying genes, such as expansins, that may be involved in differentiation of gall-specific tissues (Formiga

368 *et al.*, 2013; Suzuki *et al.*, 2015). Auxin is generally accepted to be an important regulator in gall
369 development (Tooker & Helms, 2014). Li *et al.* (2017) showed that *L. invasa* pre-larval galls accumulate
370 phenolics, tannins, flavonoids and auxins, further validating our hypothesis that components necessary
371 for gall formation are apparent within 1 dpi.
372
373 Module 2 in the network comprises numerous *L. invasa* oviposition-responsive genes (based on available
374 data) that are enriched for responses to nitrate and lipid transport (Figure 5). A number of these genes,
375 such as *3-ketoacyl-CoA synthase 1* and disease-responsive dirigent-like proteins, are involved in wax
376 biosynthesis, cuticle development and cell wall modifications, respectively (Kosma *et al.* 2010).
377 Microscopy and ultrastructural studies of the wheat-Hessian fly interaction revealed a widespread
378 increase in plant surface porosity (Kosma *et al.* 2010). These modifications may facilitate nutrient
379 accumulation in the surrounding cells that form the nutritive tissue, such as observed in the immature gall
380 (Figure 2).
381
382 Gallers are known to modify the source-sink relationship of their hosts, often resulting in increased
383 availability of sugars, lipids and proteins in the nutritive tissue of the gall chamber (Saltzmann *et al.*, 2008;
384 Nabity *et al.*, 2013; Huang *et al.*, 2014; Ferreira *et al.*, 2015). Here, transcriptional responses suggest that
385 *L. invasa* egg and oviposition can manipulate the host's metabolism as early as 1 dpi. Genes involved in
386 carbohydrate metabolism and nitrate transport are up-regulated at 1 dpi. Module 1 includes numerous
387 genes involved in carbon and nitrogen metabolism. These results are supported by Li *et al.* (2017) *L. invasa*
388 induced significant increases in carbon and nitrogen concentrations in pre-larval galls.
389
390 We observed the redifferentiation of vascular tissue into gall-specific cells at 7 dpi (Figure 2B). The
391 orientation of this dividing zone parallel to the oviposition fluid suggests that the oviposition fluid contains

392 elicitors that stimulate cell division. Where eggs are present, immature gall chambers are formed around
393 the embryo. Numerous plant-galler interactions describe the larva as the life stage that is involved in gall
394 formation; however, egg- and oviposition fluid-induced cell division in host tissues has been previously
395 reported (Leggo & Shorthouse, 2006; Sliva & Shorthouse, 2006) and causes the formation of a complete
396 gall in at least one instance (Barnewall & de Clerck-Floate, 2012). This is the first case of egg- and
397 oviposition fluid-induced gall formation for Hymenoptera.

398

399 *Coordination of the defence response*

400

401 The results suggest that ABA, JA and ET are particularly involved in regulating the *Eucalyptus-L. invasa*
402 interaction. The JA signalling pathway is considered to be the major regulator of plant-insect interactions,
403 including initial oviposition and later larval life stages (Erb & Reymond, 2019). Furthermore, JA also plays
404 an important role in the wounding response, an unavoidable consequence of many oviposition behaviours
405 (Reymond, 2013). Here, one of the enriched TF subfamilies, *MYC2*, is a master regulator of the JA pathway
406 and of the crosstalk between various phytohormone signalling cascades (Kazan & Manners, 2013).
407 Additionally, both *WRKY28* and *WRKY75* have been shown to promote plant resistance through JA/ET-
408 dependent signaling pathways (Wu & Wang, 2011; Chen *et al.*, 2013).

409

410 The plant must correctly integrate different signals to elicit an appropriate response (Jones & Dangl, 2006).
411 *EgrWRKY6* may provide one route for consolidating recognition signals in this interaction. Three
412 *EgrWRKY6s* are located in module 1 which is enriched for WRKY binding sites in the promoters of the co-
413 expressed genes suggesting an important regulatory role for this subfamily in response to *L. invasa*
414 oviposition. In *Nicotiana attenuata*, this gene differentiates wounding from *Manduca sexta* feeding
415 following recognition of oral elicitors and potentiates JA levels and defences during extended herbivore

416 attack (Skibbe *et al.*, 2008). These TFs may function similarly in this interaction by prioritising an insect-
417 specific response.
418
419 Two enriched MYB transcription factor subfamilies, *EgrMYB102* and *EgrMYB36*, were identified. *Myzus*
420 *persicae* (green peach aphid) feeding on *A. thaliana* induced expression of *MYB102* resulting in ET-
421 dependent susceptibility to aphids (Zhu *et al.*, 2018). However, over-expression of *AtMYB102* promoted
422 resistance following *Pieris rapae* (cabbage white butterfly) feeding and functions by integrating
423 dehydration signals caused by caterpillar-induced wounding (Denekamp & Smeekens, 2003; De Vos *et al.*,
424 2006). *AtMYB102* induced the expression of defence- and cell wall modification-related genes (De Vos *et*
425 *al.*, 2006). In the second case, *At*MYB36 has been shown to be responsible for directing the expression of
426 genes necessary to correctly position and deposit lignin to build Casparian strips in roots (Kamiya *et al.*,
427 2015). Interestingly, ectopic expression of *AtMYB36* is sufficient to synthesise Casparian strips in plant
428 tissues that do not normally possess these structures (Kamiya *et al.*, 2015). *AtMYB36* has also been shown
429 to regulate the transition from cell proliferation to differentiation in roots (Liberman *et al.*, 2015). Module
430 2 of the network includes three *EgrMYB102* orthologs as well as *EgrMYB36* co-expressed with genes
431 related to wax, cuticle and cell wall modifications and 83% of the genes show *L. invasa*-induced differential
432 expression based on currently available data. This suggests that module 2 may be involved in the cell wall
433 adjustment that is crucial for gall development.
434
435 The plant cell wall also serves as one of the earliest barriers encountered by pests and pathogens (Erb &
436 Reymond, 2019). Two of the enriched TF subfamilies, *MYB102* and *MYB15*, have been shown to regulate
437 basal immunity by promoting cell wall reinforcement during biotic stresses (Denekamp & Smeekens, 2003;
438 De Vos *et al.*, 2006; Chezem *et al.*, 2017).
439

440 ABA is the primary regulator of responses to dehydration which is linked to wounding that causes localised
441 water loss (Reymond, 2013). ABA also functions synergistically with JA in mediating plant defence against
442 insects (Ton *et al.*, 2009). The enriched TF subfamily, *EgrATAF1*, promotes ABA-dependent biotic stress
443 resistance but suppresses ABA-dependent abiotic stress resistance (Ton *et al.*, 2009). *EgrATAF1*-encoding
444 genes are co-expressed with genes enriched for defence related GO terms and closely correlated with
445 *EgrRAP2.1*, which is a drought-inducible, negative regulator of dehydration-responsive elements and
446 ensures fine-tuning of *A. thaliana* abiotic responses. However, Li *et al.* (2017) showed that ABA
447 concentrations are significantly increased in *L. invasa*-infested plants throughout gall development (pre-
448 larval to mature galls) which supports the genes related to ABA responses observed throughout this study.
449 This suggests that ABA participates in *L. invasa* susceptibility, possibly by preventing desiccation of the
450 egg and surrounding tissues.
451
452 These results provide a detailed insight into the early transcriptional and morphological responses of
453 *Eucalyptus* to *L. invasa* oviposition. This study significantly improved upon the current model of this
454 interaction by identifying JA, ABA, ET and ten TF subfamilies that putatively regulate the interaction.
455 Functional studies will be required to further evaluate their roles in resistance. We demonstrate that the
456 egg and oviposition fluid initiate gall development possibly by redirecting plant defence-related functions
457 with elicitors. Proteomics and/or metabolomic studies may provide a means for identifying these elicitors
458 and understanding the mechanisms behind plant-galling insect interactions.
459
460 **Acknowledgements**
461
462 We acknowledge the following people for their contributions to the study. Plant material and insectarium
463 facilities were provided by Mondi and the Forestry and Agricultural Biotechnology Institute (FABI). We

thank Ms Samantha Bush, Mr Joseph Khadile and Mr Celani Nkosi for assistance in collecting infested material and sorting wasps and Dr Krzysztof Polanski for assistance with the bioinformatics analyses.

References

Atkin O.K., Botman B. & Lambers H. (1996). The relationship between the relative growth rate and nitrogen economy of alpine and lowland Poa species. *Plant, Cell and Environment*, 19(11), 1324-1330.

Ament K., Kant M.R., Sabelis M.W., Haring M.A. & Schuurink R.C. (2004). Jasmonic Acid Is a Key Regulator of Spider Mite-Induced Volatile Terpenoid and Methyl Salicylate Emission in Tomato. *Plant Physiology* 135: 2025–2037.

Andrews S.F. (2014). A quality control tool for high throughput sequence data. Babraham Bioinformatics.

Balbyshev N.F., Lorenzen J.H. (1997). Hypersensitivity and egg drop: A novel mechanism of host-plant resistance to Colorado potato beetle (Coleoptera: Chrysomelidae). *Journal of Economic Entomology* 90: 652–657.

Barnewall E.C. & de Clerck-Floate R.A. (2012). A preliminary histological investigation of gall induction in an unconventional galling system. *Arthropod-Plant Interactions* 6: 449–459.

Bedetti C.S., Modolo L.V. & Isaias R.M. dos S. (2014). The role of phenolics in the control of auxin in galls of *Piptadenia gonoacantha* (Mart.) MacBr (Fabaceae: Mimosoideae). *Biochemical Systematics and Ecology* 55: 53–59.

Benjamini Y. & Hochberg Y. (1995). Controlling the False Discovery Rate: A Practical and Powerful Approach to Multiple Testing. *Source Journal of the Royal Statistical Society. Series B (Methodological) Journal of the Royal Statistical Society. Series B J. R. Statist. Soc. B* 57: 289–300.

Berens M.L., Berry H.M., Mine A., Argueso C.T. & Tsuda K. (2017). Evolution of Hormone Signaling

488 Networks in Plant Defense. *Annual Review of Phytopathology* 55: 401–425.
489 Berlyn G., Miksche J. & Sass J. (1976). Botanical microtechnique and cytochemistry. *Iowa State University*
490 *Press*: 326.
491 Bolger A.M., Lohse M. & Usadel B. (2014). Trimmomatic: A flexible trimmer for Illumina sequence data.
492 *Bioinformatics* 30: 2114–2120.
493 Boller T. & Felix G. (2009). A Renaissance of Elicitors: Perception of Microbe-Associated Molecular Patterns
494 and Danger Signals by Pattern-Recognition Receptors. *Annual Review of Plant Biology* 60: 379–
495 406.
496 Büchel K., McDowell E., Nelson W., Descour A., Gershenzon J., Hilker M., Soderlund C., Gang D.R., Fenning
497 T. & Meiners T. (2012). An elm EST database for identifying leaf beetle egg-induced defense genes.
498 *BMC Genomics* 13: 1–17.
499 Carocha V., Hefer C., Cassan-Wang H., Fevereiro P., Myburg A.A., Paiva J.A.P. & Grima-Pettenati J. (2015).
500 Genome-wide analysis of the lignin toolbox of *Eucalyptus grandis*. *New Phytologist* 206: 1297–
501 1313.
502 Chen X., Liu J., Lin G., Wang A., Wang Z. & Lu G. (2013). Overexpression of *AtWRKY28* and *AtWRKY75* in
503 *Arabidopsis* enhances resistance to oxalic acid and *Sclerotinia sclerotiorum*. *Plant Cell Reports* 32:
504 1589-1599.
505 Chezem W.R., Memon A., Li F-S., Weng J-K. & Clay N.K. (2017). SG2-Type R2R3-MYB Transcription Factor
506 MYB15 Controls Defense-Induced Lignification and Basal Immunity in *Arabidopsis*. *The Plant Cell*
507 29: 1907–1926.
508 Choi C., Park S., Ahn I., Bae S. & Hwang D.J. (2016). Generation of Chinese cabbage resistant to bacterial
509 soft rot by heterologous expression of Arabidopsis WRKY75. *Plant Biotechnology Reports* 5: 301-
510 307.
511 Considine M.J. & Foyer C.H. (2014). Redox Regulation of Plant Development. *Antioxidants & Redox*

512 *Signaling* 21: 1305–1326.
513 Denekamp M. & Smeekens S.C. (2003). Integration of Wounding and Osmotic Stress Signals Determines
514 the Expression of the *AtMYB102* Transcription Factor Gene. *Plant Physiology* 132: 1415–1423.
515 Deslandes L. & Rivas S. (2012). Catch me if you can: bacterial effectors and plant targets. *Trends in Plant*
516 *Science* 17: 644–655.
517 Dittrich-Schröder G., Wingfield M.J., Hurley B.P. & Slippers B. (2012). Diversity in *Eucalyptus* susceptibility
518 to the gall-forming wasp *Leptocybe invasa*. *Agricultural and Forest Entomology* 14: 419–427.
519 Dittrich-Schröder G., Hoareau T.B., Hurley B.P., Wingfield M.J., Lawson S., Nahrung H. & Slippers B. (2018).
520 Population genetic analyses of complex global insect invasions in managed landscapes: a
521 *Leptocybe invasa* (Hymenoptera) case study. *Biological Invasions* 20: 2395-2420.
522 Doss R.P., Oliver J.E., Proebsting W.M., Potter S.W., Kuy S., Clement S.L., Williamson R.T., Carney J.R. &
523 DeVilbiss E.D. (2000). Bruchins: Insect-derived plant regulators that stimulate neoplasm
524 formation. *Proceedings of the National Academy of Sciences* 97: 6218–6223.
525 Erb M., Meldau S. & Howe G.A. (2012). Role of phytohormones in insect-specific plant reactions. *Trends*
526 *in Plant Science* 17: 250–259.
527 Erb M. & Reymond P. (2019). Molecular interactions between plants and insect herbivores. *Annual Review*
528 *of Plant Biology* 70: 527-557.
529 Ferreira B.G., Carneiro R.G.S. & Isaias R.M.S. (2015). Multivesicular bodies differentiate exclusively in
530 nutritive fast-dividing cells in *Marcetia taxifolia* galls. *Protoplasma* 252: 1275–1283.
531 Formiga A.T., de Oliveira D.C., Ferreira B.G., Magalhães T.A., de Castro A.C., Fernandes G.W., Isaias R.M.
532 dos S. (2013). The role of pectic composition of cell walls in the determination of the new shape-
533 functional design in galls of *Baccharis reticularia* (Asteraceae). *Protoplasma* 250: 899–908.
534 Fürstenberg-Hägg J., Zagrobelny M. & Bak S. (2013). Plant Defense against Insect Herbivores. *International*
535 *Journal of Molecular Sciences* 14: 10242–10297.

536 Geuss D., Stelzer S., Lortzing T. & Steppuhn A. (2017). *Solanum dulcamara*'s response to eggs of an insect
537 herbivore comprises ovicidal hydrogen peroxide production. *Plant, Cell & Environment* 40: 2663–
538 2677.
539 Giron D., Huguet E., Stone G.N. & Body M. (2016). Insect-induced effects on plants and possible effectors
540 used by galling and leaf-mining insects to manipulate their host-plant. 84: 70–89.
541 Gouhier-Darimont C., Schmiesing A., Bonnet C., Lassueur S. & Reymond P. (2013). Signalling of *Arabidopsis*
542 *thaliana* response to *Pieris brassicae* eggs shares similarities with PAMP-triggered immunity.
543 *Journal of Experimental Botany* 64: 665–674.
544 Griese E., Dicke M., Hilker M. & Fatouros N.E. (2017). Plant response to butterfly eggs: inducibility, severity
545 and success of egg-killing leaf necrosis depends on plant genotype and egg clustering. *Scientific*
546 *Reports* 7: 1–12.
547 Guo P., Li Z., Huang P., Li B., Fang S., Chu J. & Guo H. (2017). A tripartite amplification loop involving the
548 transcription factor WRKY75, salicylic acid and reactive oxygen species accelerates leaf
549 senescence. *The Plant Cell* 29: 2854-2870.
550 Hall C.R., Carroll A.R., Kitching R.L. (2017). A meta-analysis of the effects of galling insects on host plant
551 secondary metabolites. *Arthropod-Plant Interactions* 11: 463–473.
552 Hilker M. & Fatouros N.E. (2015). Plant Responses to Insect Egg Deposition. *Annual Review of Entomology*
553 60: 493–515.
554 Hilker M. & Fatouros N.E. (2016). Resisting the onset of herbivore attack: Plants perceive and respond to
555 insect eggs. *Current Opinion in Plant Biology* 32: 9–16.
556 Hilker M., Kobs C., Varama M. & Schrank K. (2002). Insect egg deposition induces *Pinus sylvestris* to attract
557 egg parasitoids. *The Journal of Experimental Biology* 205: 455–461.
558 Hogenhout S.A. & Bos J.I.B. (2011). Effector proteins that modulate plant-insect interactions. *Current*
559 *Opinion in Plant Biology* 14: 422–428.

560 Huang M.Y., Huang W.D., Chou H.M., Lin K.H., Chen C.C., Chen P.J., Chang Y.T. & Yang C.M. (2014). Leaf-
561 derived cecidomyiid galls are sinks in *Machilus thunbergii* (Lauraceae) leaves. *Physiologia*
562 *Plantarum* 152: 475–485.
563 Isaias R.M. dos S, Ferreira B.G., Alvarenga D.R. de, Barbosa L.R., Salminen J.P. & Steinbauer M.J. (2018).
564 Functional compartmentalisation of nutrients and phenolics in the tissues of galls induced by
565 *Leptocybe invasa* (Hymenoptera: Eulophidae) on *Eucalyptus camaldulensis* (Myrtaceae). *Austral*
566 *Entomology* 57: 238–246.
567 Isaias R.M.S., Oliveira D.C., Moreira A.S.F.P., Soares G.L.G. & Carneiro R.G.S. (2015). The imbalance of
568 redox homeostasis in arthropod-induced plant galls: Mechanisms of stress generation and
569 dissipation. *Biochimica et Biophysica Acta* 1850: 1509–1517.
570 Jin J., He K., Tang X., Li Z., Lv L., Zhao Y., Luo J & Gao G. (2015). An *Arabidopsis* transcriptional regulatory
571 map reveals distinct functional and evolutionary features of novel transcription factors. *Molecular*
572 *Biology and Evolution* 32: 1767–1773.
573 Jin J., Tian F., Yang D.C., Meng Y.Q., Kong L., Luo J. & Gao G. (2017). PlantTFDB 4.0: Toward a central hub
574 for transcription factors and regulatory interactions in plants. *Nucleic Acids Research* 45: D1040–
575 D1045.
576 Jin J., Zhang H., Kong L., Gao G. & Luo J. (2014). PlantTFDB 3.0: A portal for the functional and evolutionary
577 study of plant transcription factors. *Nucleic Acids Research* 42: 1182–1187.
578 Jones J.D.G. & Dangl J.L. (2006). The plant immune system. *Nature* 444: 323–329.
579 Kamiya T., Borghi M., Wang P., Danku J.M., Kalmbach L., Hosmani P.S., Naseer S., Fujiwara T., Geldner N.
580 & Salt D.E. (2015). The MYB36 transcription factor orchestrates Casparian strip formation.
581 *Proceedings of the National Academy of Sciences* 112: 10533-10538.
582 Kazan K. & Manners J.M. (2013). MYC2: The master in action. *Molecular Plant* 6: 686–703.
583 Kim D., Pertea G., Trapnell C., Pimentel H., Kelley R. & Salzberg SL. (2013). TopHat2: Accurate alignment

584 of transcriptomes in the presence of insertions, deletions and gene fusions. *Genome Biology* 14:
585 R36.
586 Kosma D.K., Nemacheck J.A., Jenks M.A. & Williams C.E. (2010). Changes in properties of wheat leaf cuticle
587 during interactions with Hessian fly. *The Plant Journal* 63:31-43.
588 Leggo J.J. & Shorthouse J.D. (2006b). Development of stem galls induced by *Diplolepis triforma*
589 (Hymenoptera: Cynipidae) on *Rosa acicularis* (Rosaceae). *Canadian Entomologist* 138: 661–680.
590 Li X.Q., Liu Y.Z., Guo W.F., Solanki M.K., Yang Z.D., Xiang Y., Ma Z.C. & Wen Y.G. (2017). The gall wasp
591 *Leptocybe invasa* (Hymenoptera: Eulophidae) stimulates different chemical and phytohormone
592 responses in two *Eucalyptus* varieties that vary in susceptibility to galling. *Tree Physiology* 37:
593 1208–1217.
594 Liao Y., Smyth G.K. & Shi W. (2014). FeatureCounts: An efficient general purpose program for assigning
595 sequence reads to genomic features. *Bioinformatics* 30: 923–930.
596 Liberman L.M., Sparks E.E., Moreno-Risueno M.A., Petricka J.J., Benfey P.N. (2015). MYB36 regulates the
597 transition from proliferation to differentiation in the *Arabidopsis* root. *Proceedings of the National*
598 *Academy of Sciences* 112: 12099-12104.
599 Little D., Gouhier-Darimont C., Bruessow F. & Reymond P. (2006). Oviposition by Pierid Butterflies Triggers
600 Defense Responses in *Arabidopsis*. *Plant Physiology* 143: 784–800.
601 Love M.I., Huber W. & Anders S. (2014). Moderated estimation of fold change and dispersion for RNA-seq
602 data with DESeq2. *Genome Biology* 15: 1–21.
603 Mangwanda R., Myburg A.A. & Naidoo S. (2015). Transcriptome and hormone profiling reveals *Eucalyptus*
604 *grandis* defence responses against *Chrysoporthe austroafricana*. *BMC Genomics* 16: 1–13.
605 Mendel Z., Protasov A., Fisher N. & La Salle J. (2004). Taxonomy and biology of *Leptocybe invasa* gen. &
606 sp. n. (Hymenoptera: Eulophidae), an invasive gall inducer on *Eucalyptus*. *Australian Journal of*
607 *Entomology* 43: 101–113.

608 Meyer F.E., Shuey L.S., Naidoo S., Mamni T., Berger D.K., Myburg A.A., van den Berg N. & Naidoo S. (2016).
609 Dual RNA-Sequencing of *Eucalyptus nitens* during *Phytophthora cinnamomi* Challenge Reveals
610 Pathogen and Host Factors Influencing Compatibility. *Frontiers in Plant Science* 7: 1–15.
611 Morris J.H., Apeltsin L., Newman A.M., Baumbach J, Wittkop T., Su G., Bader G.D. & Ferrin T.E. (2011).
612 ClusterMaker: A multi-algorithm clustering plugin for Cytoscape. *BMC Bioinformatics* 12: 436.
613 Myburg A.A., Grattapaglia D., Tuskan G.A., Hellsten U., Hayes R.D., Grimwood J., Jenkins J., Lindquist E.,
614 Tice H., Bauer D., *et al.* (2014). The genome of *Eucalyptus grandis*. *Nature* 510: 356–362.
615 Nabity P.D., Haus M.J., Berenbaum M.R. & DeLucia E.H. (2013). Leaf-galling phylloxera on grapes
616 reprograms host metabolism and morphology. *Proceedings of the National Academy of Sciences*
617 110: 16663–16668.
618 Oates C.N., Denby K.J., Myburg A.A., Slippers B. & Naidoo S. (2016). Insect Gallers and Their Plant Hosts:
619 From Omics Data to Systems Biology. *International Journal of Molecular Sciences* 17.
620 Oates C.N., Külheim C., Myburg A.A., Slippers B. & Naidoo S. (2015). The Transcriptome and Terpene
621 Profile of *Eucalyptus grandis* Reveals Mechanisms of Defense Against the Insect Pest, *Leptocybe*
622 *invasa*. *Plant and Cell Physiology* 56: 1418–1428.
623 R Core Team (2018). R: A language and environment for statistical computing. R Foundation for Statistical
624 Computing, Vienna, Austria. URL https://www.R-project.org/.
625 Reymond P. (2013). Perception, signaling and molecular basis of oviposition-mediated plant responses.
626 *Planta* 238: 247–258.
627 Saltzmann K.D., Giovanini M.P., Zheng C., & Williams C.E. (2008). Virulent Hessian Fly Larvae Manipulate
628 the Free Amino Acid Content of Host Wheat Plants. *Journal of Chemical Ecology* 34: 1401–1410.
629 Shannon P., Markiel A., Ozier O., Baliga N.S., Wang J.T., Ramage D., Amin N., Schwikowski B. & Ideker T.
630 (2003). Cytoscape: A software Environment for integrated models of biomolecular interaction
631 networks. *Genome Research* 13: 2498–2504.

632 Skibbe M., Qu N., Galis I. & Baldwin I.T. (2008). Induced Plant Defenses in the Natural Environment: 633 *Nicotiana attenuata* WRKY3 and WRKY6 Coordinate Responses to Herbivory. *the Plant Cell Online* 634 20: 1984–2000.

635 Sliva M.D. & Shorthouse J.D. (2006). Comparison of the development of stem galls induced by *Aulacidea* 636 *hieracii* (Hymenoptera : Cynipidae) on hawkweed and by *Diplolepis spinosa* (Hymenoptera : 637 Cynipidae) on rose. *Canadian Journal of Botany-Revue Canadienne de Botanique* 84: 1052–1074.

638 Stone G.N. & Schönrogge K. (2003). The adaptive significance of insect gall morphology. *Trends in Ecology* 639 *and Evolution* 18: 512–522.

640 Stuart J. (2015). Insect effectors and gene-for-gene interactions with host plants. *Current Opinion in Insect* 641 *Science* 9: 56–61.

642 Suzuki A.Y.M., Bedetti C.S. & Isaias R.M. dos S. (2015). Detection and distribution of cell growth regulators 643 and cellulose microfibrils during the development of Lopesia sp. galls on *Lonchocarpus cultratus* 644 (Fabaceae). *Botany* 93: 435–444.

645 Takeda S., Yoza M., Amano T., Ohshima I., Hirano T., Sato M.H., Sakamoto T. & Kimura S. (2019). 646 Comparative transcriptome analysis of galls from four different host plants suggests the molecular 647 mechanism of gall development. *PloS one*10.

648 Ton J., Flors V. & Mauch-Mani B. (2009). The multifaceted role of ABA in disease resistance. *Trends in Plant* 649 *Science* 14: 310–317.

650 Tooker J.F. & Helms A.M. (2014). Phytohormone Dynamics Associated with Gall Insects, and their Potential 651 Role in the Evolution of the Gall-Inducing Habit. *Journal of Chemical Ecology* 40: 742–753.

652 Tzfadia O., Diels T., De Meyer S., Vandepoele K., Aharoni A. & Van de Peer Y. (2016). CoExpNetViz: 653 Comparative Co-Expression Networks Construction and Visualization Tool. *Frontiers in Plant* 654 *Science* 6: 1–7.

655 Unsicker S.B., Kunert G. & Gershenzon J. (2009). Protective perfumes: the role of vegetative volatiles in

656 plant defense against herbivores. *Current Opinion in Plant Biology* 12: 479–485.
657 De Vos M., Denekamp M., Dicke M., Vuylsteke M., Van Loon LC, Smeekens S.C.M. & Pieterse C.M.J. (2006).
658 The *Arabidopsis thaliana* transcription factor AtMYB102 functions in defense against the insect
659 herbivore *Pieris rapae*. *Plant Signaling and Behavior* 1: 305–311.
660 Wu P. & Wang Z. (2011). Molecular mechanisms regulating Pi-signaling and Pi homeostasis under OsPHR2,
661 a central Pi-signaling regulator, in rice. *Frontiers in Biology* 6: 242-245.
662 Zhu L., Guo J., Ma Z., Wang J. & Zhou C. (2018). *Arabidopsis* transcription factor MYB102 increases plant
663 susceptibility to aphids by substantial activation of ethylene biosynthesis. *Biomolecules* 8.
664
665

666 **Figure Legends**

667

668 **Figure 1. Methodological overview of the *L. invasa* infestation** applied to susceptible *Eucalyptus grandis*
669 x *E. camaldulensis* ramets to obtain one biological replicate at a single time point of infested and control
670 samples. (**A**) Three target sites (shoot tip, first and second leaves as well as their respective petioles,
671 indicated in blocks) were selected per ramet. Each target site was exposed to five, newly emerged *L.*
672 *invasa* females (infested) from 11:00 to 12:00 to minimise diurnal variation. Wasp movement was
673 restricted using plastic bags enclosed around the target sites. Material was excised approximately 5 mm
674 around the oviposition scars (dotted lines). Each biological replicate (BR1) comprised pooled material from
675 three different ramets (Ramet 1, 2 and 3). (**B**) Control samples at 1 and 2 dpi were treated similarly with
676 empty bags enclosed around the target sites. For 1 and 2 dpi control samples, the shoot tip, midrib and
677 lower third of the midrib (dotted line) were pooled across the ramets (all potential targets where females
678 were likely to lay eggs) (**C**) For 3 dpi controls, the shoot tip (top), midrib (middle) and petiole (bottom)
679 were pooled separately.

680

681 **Figure 2.** *Leptocybe invasa* oviposition-induced physiological responses leading to gall development. (**A1**)
682 Oviposition occurs along the midrib and induces a necrotic response and ROS accumulation (arrows,
683 stained with DAB) within one hour. (**A2-A5**) At 1 dpi, scarring is apparent and is visible until 7 dpi. ROS
684 accumulation increases until 3 dpi with a similar intensity at 7 dpi and is co-localised with the scarred
685 tissue. (**B1, B2**) Comparisons of cross and longitudinal sections (dual-stained with Safranin O and Fast
686 Green FCF) of control tissue at 7 dpi versus (**B3-B5**) infested tissue indicate that eggs are deposited singly
687 into the vasculature in an alternating pattern, ie. alternately on the left and right side of the midrib. The
688 oviposition fluid (red-stained fluid) is spread throughout the oviposition site and has a rapid degradative
689 effect on the surrounding tissue. The egg is round and anchored to the tissue with a pedicle that may also

690 absorb water and nutrients from the surrounding tissue. (**B6-B8**) The egg elongates by 1 dpi and becomes
691 roughly aligned with the vascular tissue. This shape and orientation is also present at 2 and 3 dpi. Phenolic
692 accumulation (purple-stained compounds) occurs by 1 dpi proximal to the oviposition site on the ventral
693 leaf surface and is sustained over the time series. (**B9-B12**) At 7 dpi, extensive cell division is visible parallel
694 to localisation of oviposition fluid at the oviposition sites as well as proximal to the eggs in the vascular
695 tissue and decreases with distance. The developing embryos, still enclosed by the egg membrane, are
696 surrounded by dividing cells within the vasculature indicating tissue redifferentiation. An immature gall
697 has formed with the egg located in the larval chamber. (**B13**) The mature gall comprises three distinct
698 tissue layers surrounding the larva. The nutritive tissue forms the inner-most lining of the larval chamber.
699 It is approximately 5 cell layers thick and cells possess a granular cytoplasm. A lignified sheath surrounds
700 the nutritive tissue. The final layer includes oxalate crystal deposits. VT: vascular tissue, OG: oil gland, E:
701 egg, OF: oviposition fluid, OS: oviposition site, cd: cell degradation, P: pedicel, PH: phenolics, IG: immature
702 gall, div: cell division, L: larva, NT: nutritive tissue, LS: lignified sheath, OC: oxalate crystals. Blocks indicate
703 areas shown at higher magnification.
704
705 **Figure 3. *Leptocybe invasa* oviposition-induced transcriptomic responses leading to gall development.**
706 (**A1-A4**) Heatmaps showing selected GO terms of up- (red) and down-regulated (blue), significantly
707 differentially expressed genes at 1, 2 and 3 dpi (adjusted p-value ≤ 0.05). Colour bar indicates significance.
708 (**B**) The phenylpropanoid pathway indicating heat maps of the gene expression of biosynthesis-related
709 genes at 1, 2 and 3 dpi. Red indicates up-regulation, blue indicates down-regulation. Coloured boxes
710 indicate the position of the genes in the pathway. Pathway adapted from Carocha *et al.* (2015).
711
712 **Figure 4. Expression profiles of genes belonging to ten transcription factor subfamilies showing**
713 **enrichment at 1 dpi.** Heatmaps indicate the $\log_2$ (fold change) of differentially expressed transcription

714 factors as well as their absolute expression values (VST) under normal conditions in the *E. grandis* tissue
715 atlas (https://eucgenie.org). Colour bar indicates individual members of the transcription factor
716 subfamilies.
717
718 **Figure 5. Co-expression network of genes with clusters and bait genes shown.** Baits are shown as ovals,
719 *L. invasa*-responsive nodes are shown as diamonds and genes are colour-coded according to module
720 membership. Coloured blocks indicate selected overrepresented GO biological process terms and
721 enriched transcription factor binding sites for their respective modules. Orange nodes in module 1
722 represent phenylpropanoid biosynthetic genes. Edges indicate positive correlation between nodes with
723 length indicative of correlation coefficient.
724
725 **Supplementary File S1.** Microscopy images of *Leptocybe invasa* oviposition-induced physiological
726 responses.
727
728 **Supplementary File S2.** Summary of significantly differentially expressed genes and their annotations
729 identified at 1, 2 and 3 dpi, GO enrichments and phenylpropanoid metabolism related genes.
730
731 **Supplementary File S3.** Summary of significantly differentially expressed transcription factor-encoding
732 genes at 1, 2 and 3 dpi.
733
734 **Supplementary File S4.** Summary of co-expression module members, correlations and GO enrichment.
735
736 **Supplementary File S5.** Summary of enriched transcription factor binding motifs in network module 1, 2
737 and 3.

Author Contributions

CNO conceived of the study, performed all experiments, collected sample material, analysed all data, drafted the manuscript and prepared all figures. SN conceived of and supervised the study as well as helped draft the manuscript. KJD, AAM and BS helped draft the manuscript. The authors declare no conflict of interest.

Funding

This work was supported by the Department of Science and Technology grant for Forest Genomics and Biotechnology, the South African National Research Foundation Grant for Y-rated researchers [UID105767 to SN]; Incentive funding for rated researchers [UID95807]; Technology and Human Resources for Industry Programme (THRIP; Grant ID 96413); and the Technology Innovation Agency (TIA) Forest Molecular Genetics Cluster Programme. Opinions expressed and the conclusion arrived at are those of the authors and are not necessarily to be attributed to the NRF.

Disclosures

762

763 The authors have no conflicts of interest to declare.

764

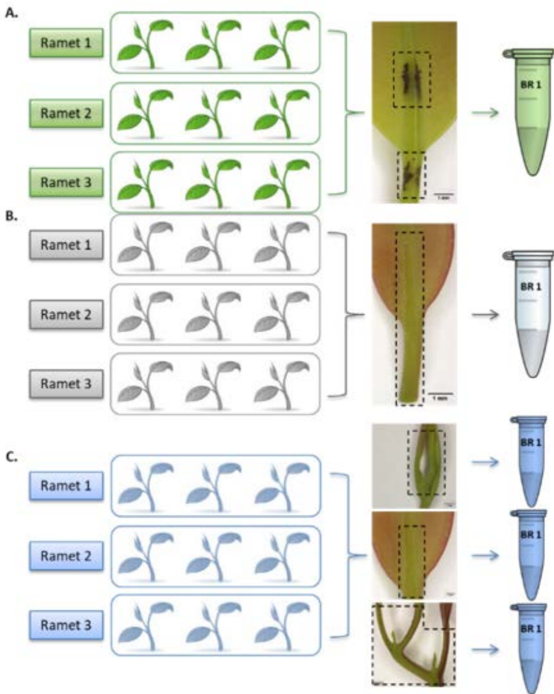
A.
Ramet 1
Ramet 2
Ramet 3
BR 1
B.
Ramet 1
Ramet 2
Ramet 3
BR 1
C.
Ramet 1
Ramet 2
Ramet 3
BR 1
BR 1
BR 1

0 dpi
1 dpi
2 dpi
3 dpi
7 dpi
Unstained
DAB

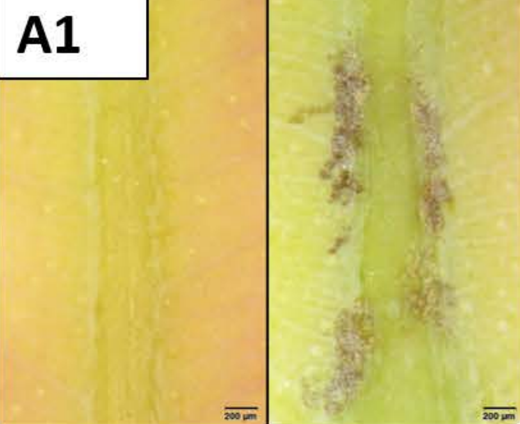
A1

A2

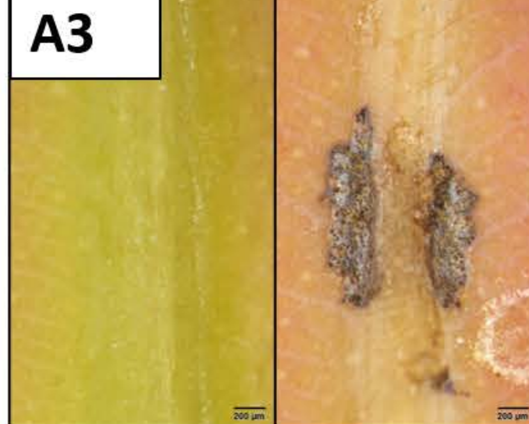
A3

A4

A5

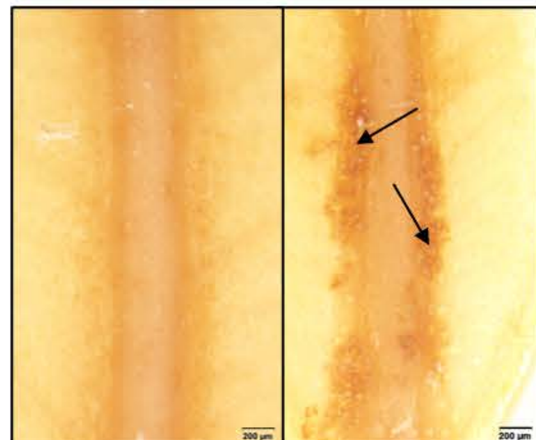

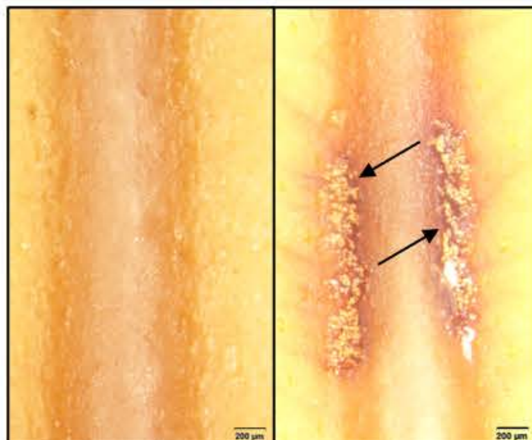

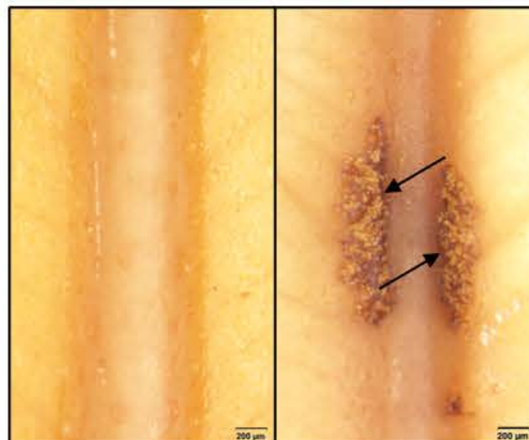

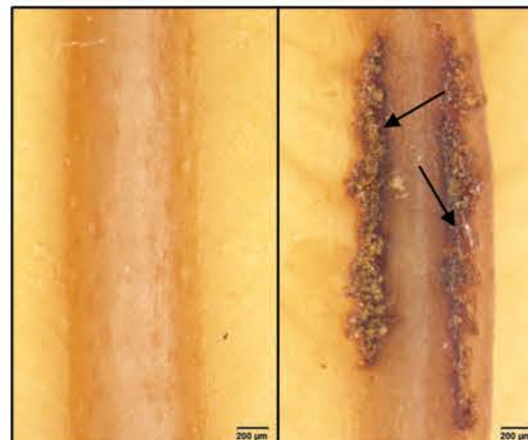

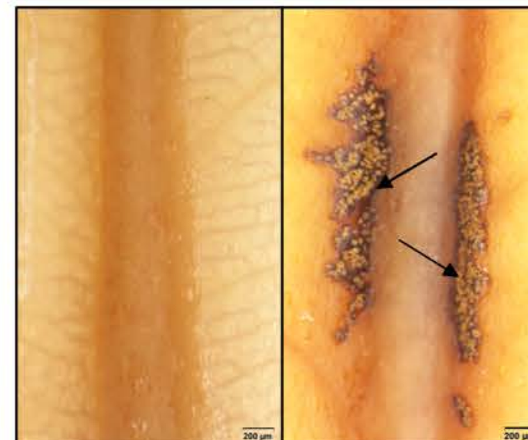

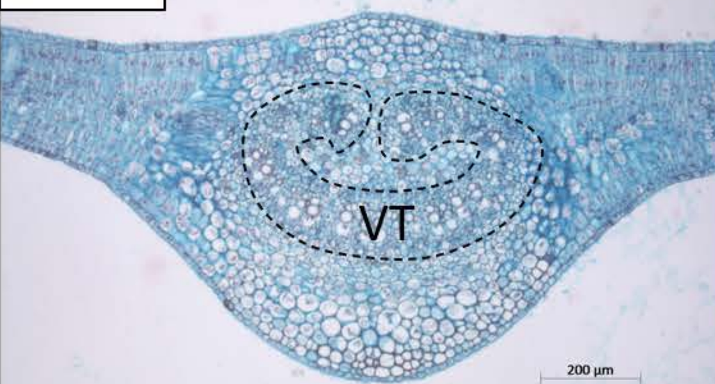
B1.
VT
200 µm

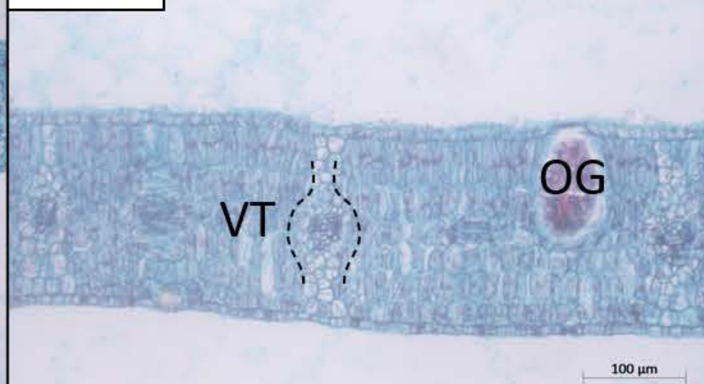
B2.
VT
OG
100 µm

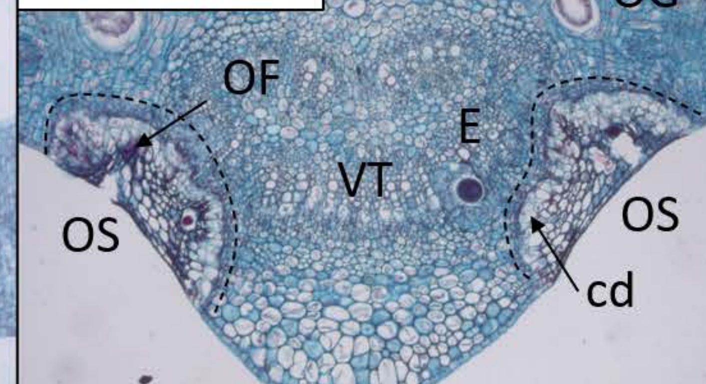
B3. 0 dpi
OG
OF
E
VT
OS
OS
cd
200 µm

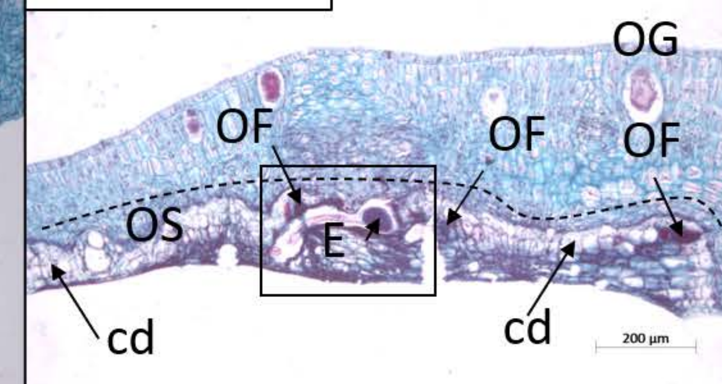
B4. 0 dpi
OG
OF
OF
OF
OS
E
cd
cd
200 µm

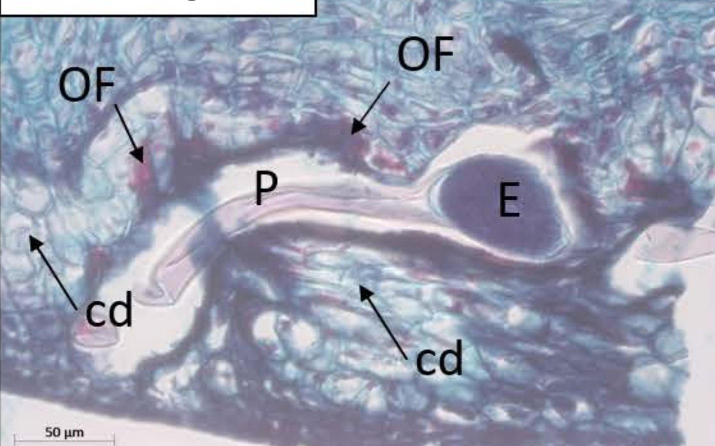
B5. 0 dpi
OF
OF
P
E
cd
cd
50 µm

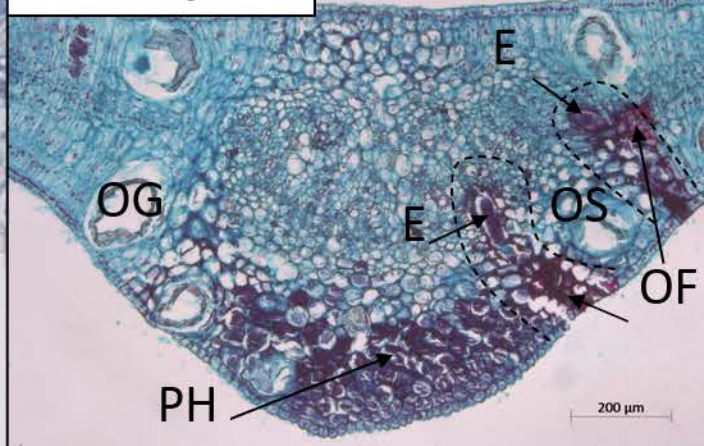
B6. 1 dpi
E
OG
E
OS
OF
PH
200 µm

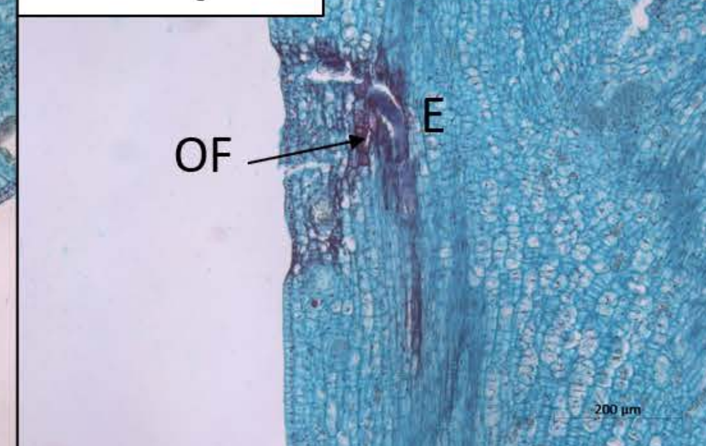
B7. 2 dpi
OF
E
200 µm

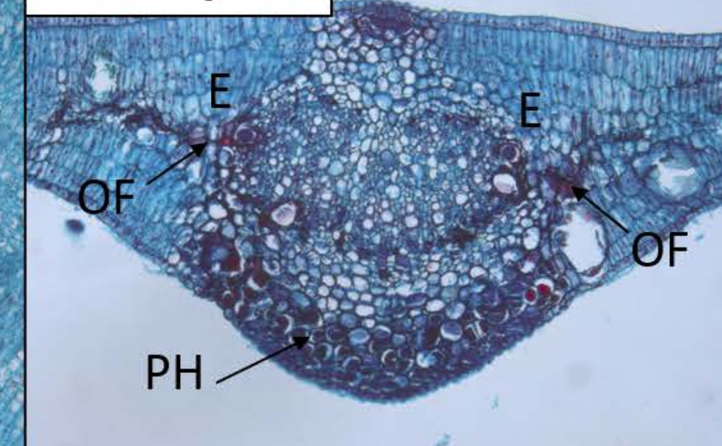
B8. 3 dpi
E
E
OF
OF
PH

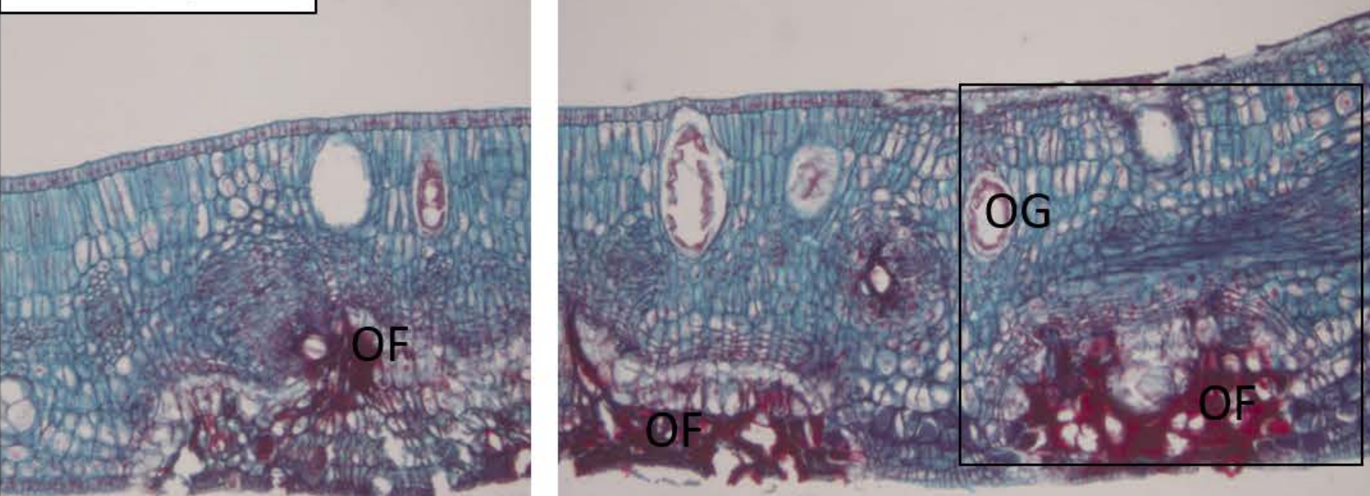
B9. 7 dpi
OF
OF
OG
OF

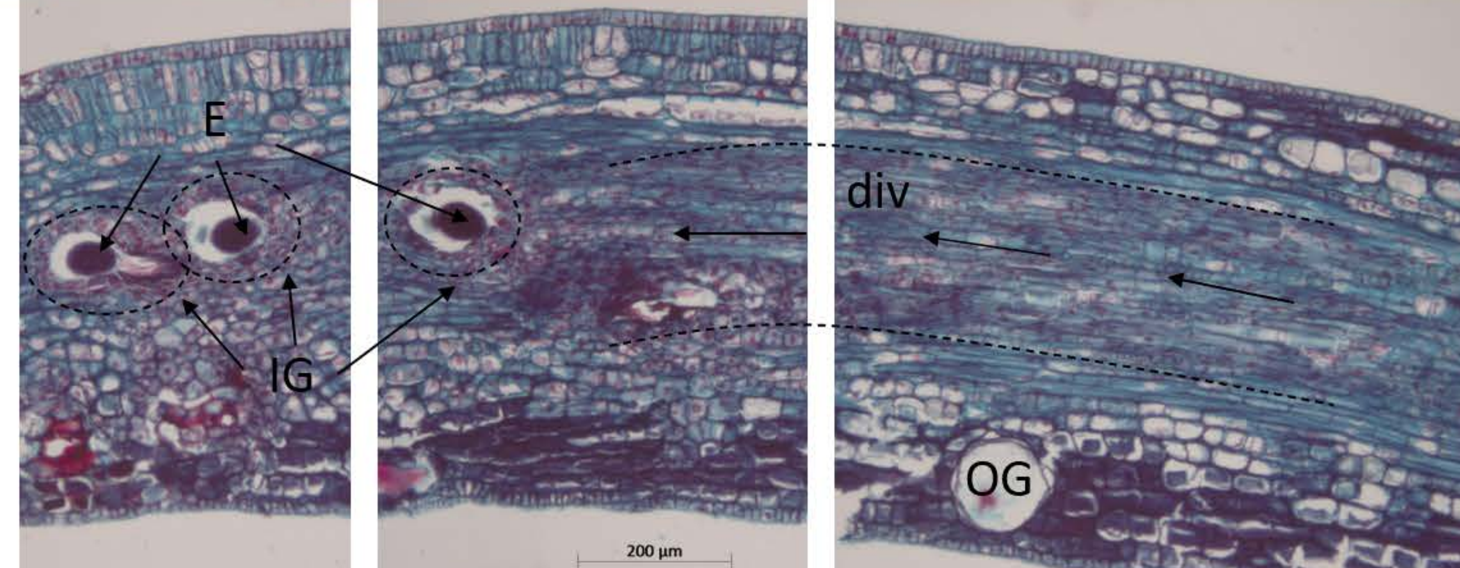
E
div
IG
OG
200 µm

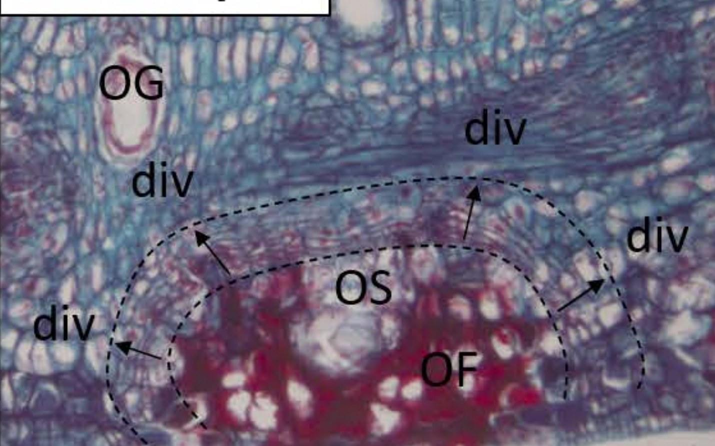
B10. 7 dpi
OG
div
div
div
div
OS
OF

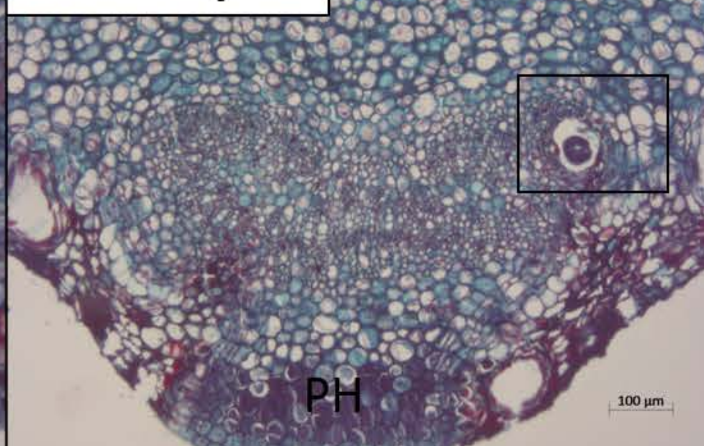
B11. 7 dpi
PH
100 µm

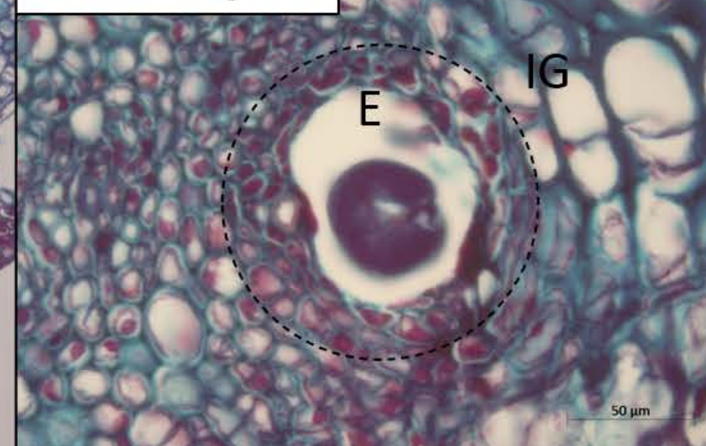
B12. 7 dpi
E
IG
50 µm

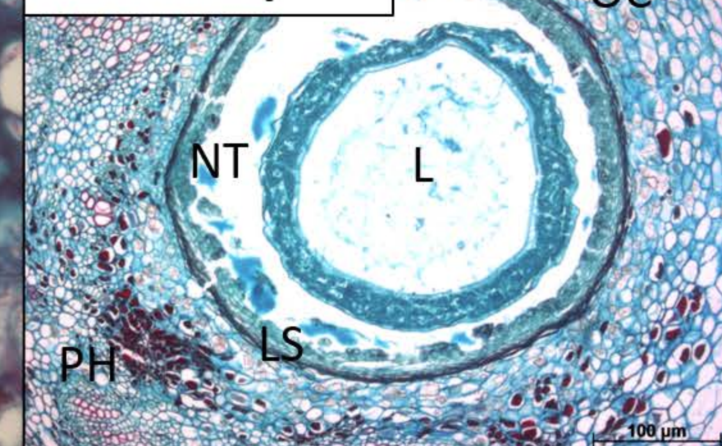
B13. 90 dpi
OC
NT
L
LS
PH
100 µm

A1. Phytohormones

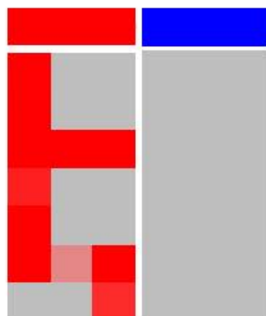

A2. Oxidative burst

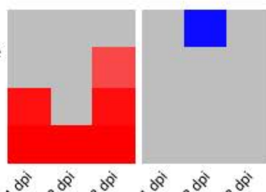

A3. Secondary metabolism

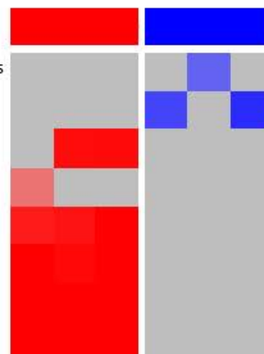

A4. Primary metabolism

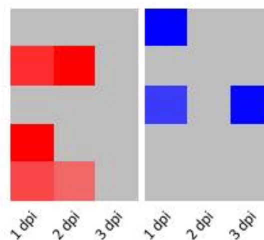

B. Phenylpropanoid Biosynthetic Pathway

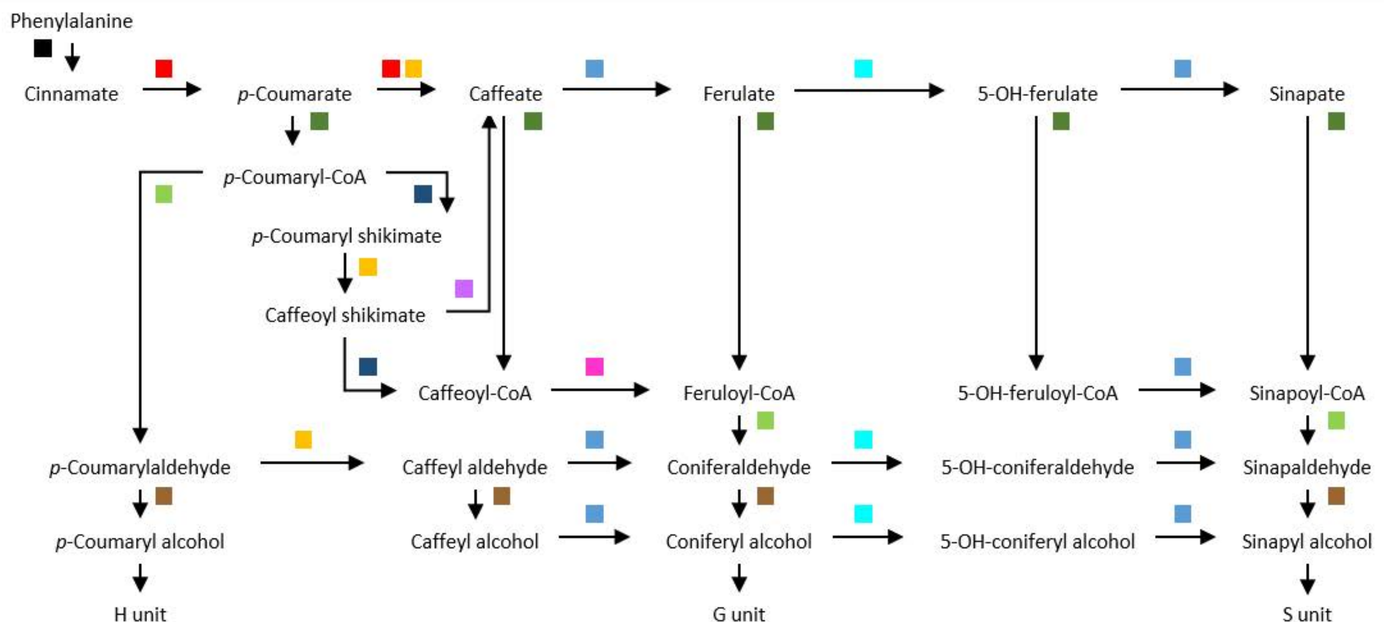

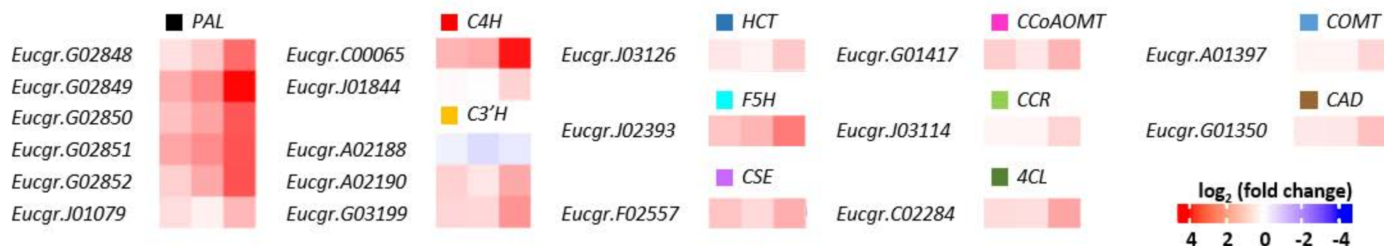

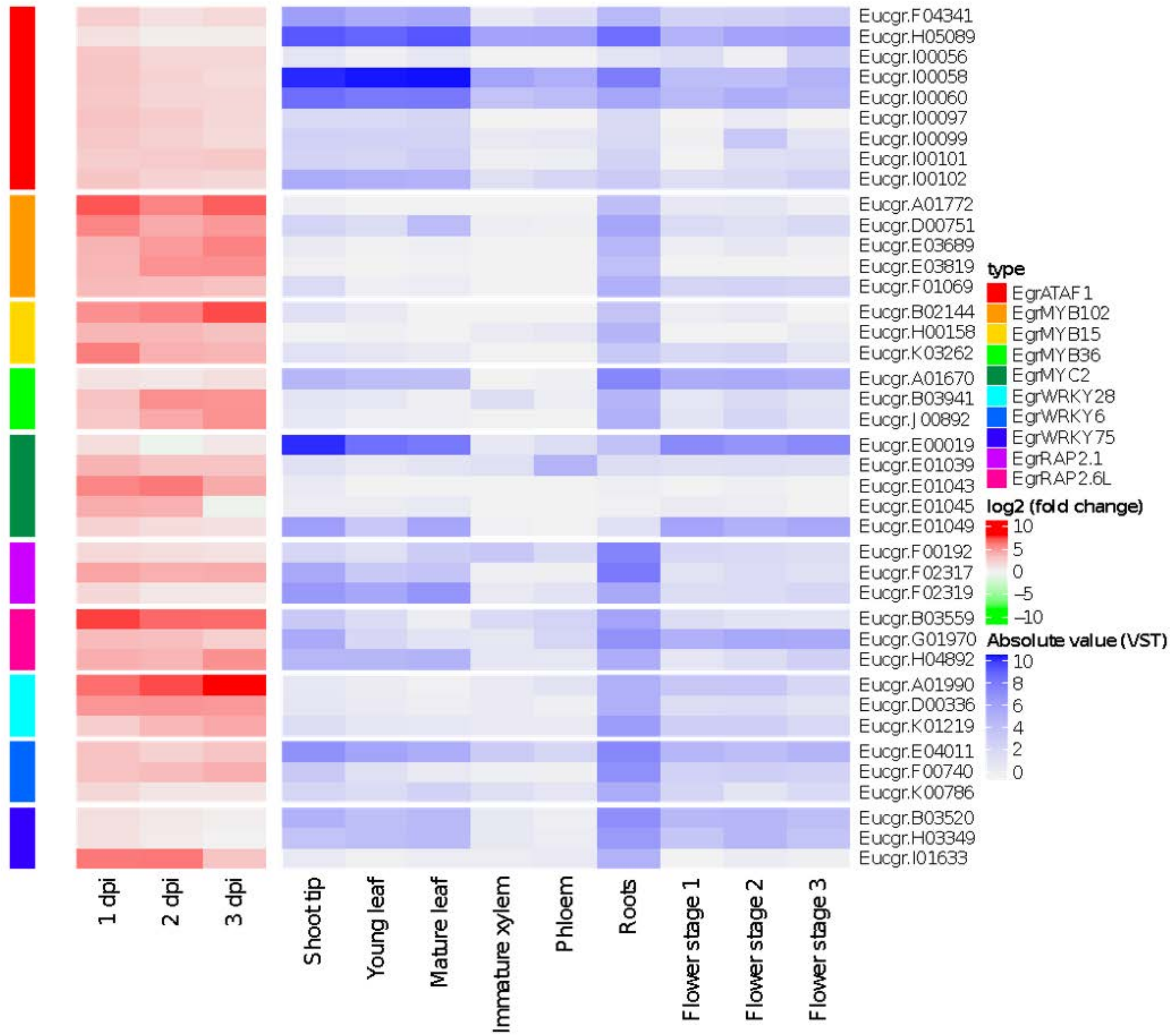
Eucgr.F04341
Eucgr.H05089
Eucgr.I00056
Eucgr.I00058
Eucgr.I00060
Eucgr.I00097
Eucgr.I00099
Eucgr.I00101
Eucgr.I00102
Eucgr.A01772
Eucgr.D00751
Eucgr.E03689
Eucgr.E03819
Eucgr.F01069
Eucgr.B02144
Eucgr.H00158
Eucgr.K03262
Eucgr.A01670
Eucgr.B03941
Eucgr.J00892
Eucgr.E00019
Eucgr.E01039
Eucgr.E01043
Eucgr.E01045
Eucgr.E01049
Eucgr.F00192
Eucgr.F02317
Eucgr.F02319
Eucgr.B03559
Eucgr.G01970
Eucgr.H04892
Eucgr.A01990
Eucgr.D00336
Eucgr.K01219
Eucgr.E04011
Eucgr.F00740
Eucgr.K00786
Eucgr.B03520
Eucgr.H03349
Eucgr.I01633
type
EgrATAF1
EgrMYB102
EgrMYB15
EgrMYB36
EgrMYC2
EgrWRKY28
EgrWRKY6
EgrWRKY75
EgrRAP2.1
EgrRAP2.6L
log2 (fold change)
10
5
0
−5
−10
Absolute value (VST)
10
8
6
4
2
0
1 dpi
2 dpi
3 dpi
Shoot tip
Young leaf
Mature leaf
Immature xylem
Phloem
Roots
Flower stage 1
Flower stage 2
Flower stage 3

Module 1	
GO terms	**Adj p-val**
❖ phenylpropanoid biosynthetic process	<0.001
❖ regulation of response to nutrient levels	0.007
❖ response to abscisic acid stimulus	<0.001
❖ response to ethylene stimulus	<0.001
❖ response to jasmonic acid stimulus	<0.001
❖ response to oxidative stress	0.001
❖ response to salicylic acid stimulus	0.04
❖ systemic acquired resistance	<0.001
Transcription factor binding sites	**E value**
○ *WRKY*	<0.001
	<0.001
	<0.001
○ *NAC*	<0.001
	<0.001

Module 2	
GO terms	**Adj p-val**
❖ lipid transport	0.003
❖ nitrate transport	0.03
❖ response to nitrate	0.02
Transcription factor binding sites	**E value**
○ *MYB*	<0.001
	<0.001
	<0.001

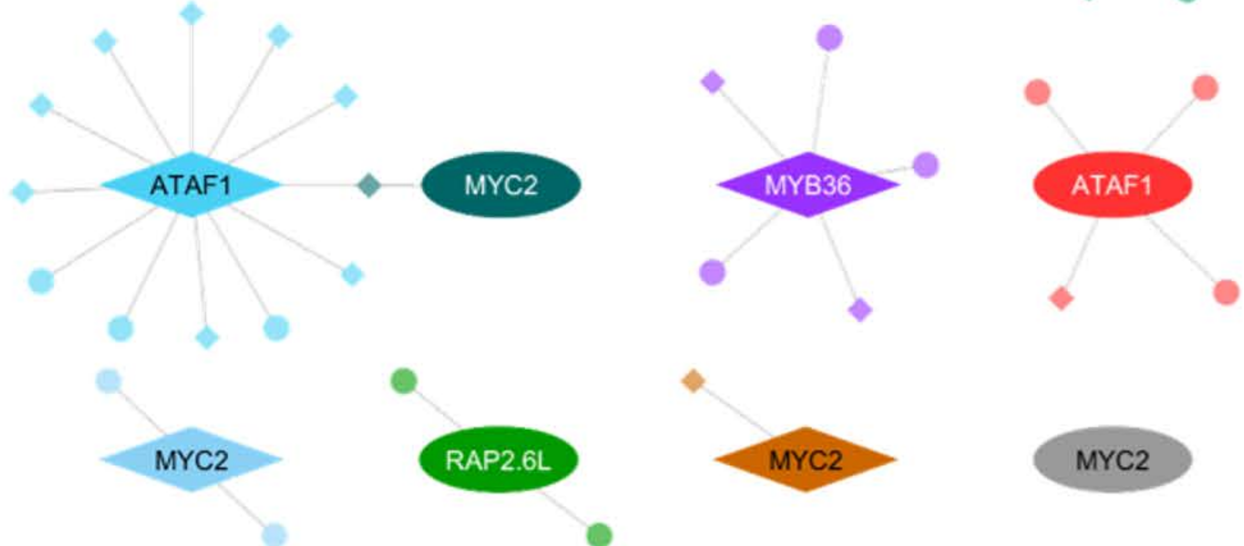

Legend

Module 1	Cluster 7	Transcription factor
Module 2	Cluster 8	Transcription factor (*Leptocybe*-specific)
Cluster 3	Cluster 9	
Cluster 4	Cluster 10	Node
Cluster 5	Cluster 11	
Cluster 6	Cluster 12	Node (*Leptocybe*-specific)